

SEPIC Based Solar Array Simulator

I. Szekely¹; L. Turos²; I. Hegyi³; G. Csern  th¹

¹Sapientia University, T  rgu Mure  , Romania

²Transilvania University, Brasov, Romania

³S.C. Gautinfo S.R.L., T  rgu Mure  , Romania

Abstract - A laboratory grade electrical photovoltaic simulator system is presented in the paper offering a viable alternative for simulating direct sunlight effects in indoor experiments. In order to validate the photovoltaic model for a single cell, the simulated characteristics were compared against the selected cell's datasheet. The SEPIC converter was chosen for its characteristics that it can cover a wide range of output voltage, including its good behavior near short circuit conditions. The SEPIC Simulink model was developed and validated by PSPICE simulation. Using the SEPIC transfer characteristics the achievable resolution has been verified and the tracking algorithm has been detailed which follows the I-V curves of the simulated solar array in different load conditions.

Keywords – SEPIC, solar array simulator, solar radiation, SIMULINK, photovoltaic cell, tracking algorithm, resolution.

1. INTRODUCTION

Since the conventional energy sources are limited and their excessive usage has negative environmental imprint, developing cleaner and ecological energy harvesting methods have an increased importance. Well known the Sun is one of our major and nearly unlimited, cleanest energy source we could explore. But given the random and cyclical nature of solar radiation energy, systems based only on solar power cannot be developed and tested in a continuous manner.

Testing these systems at night or on a cloudy day makes it difficult. We also know the solar irradiation (insolation) is a measure of solar radiation energy received on a given surface area and recorded during a given time so the solar irradiation power depends heavily on the geographical position where the solar panels are located and the time of the year and/or time of the day when it is considered. Beside these parameters a solar energy harvesting system has several other parameters that affect the harvesting system efficiency such as ambient temperature variations, orientation of the panels, the photovoltaic cell's efficiency, the electronic converter's efficiency, wiring losses, poor maintenance of photovoltaic cells, and dust and grime collection on the photovoltaic modules.

Overcoming all these negative factors in a development process we planned to elaborate a laboratory grade, electrical photovoltaic simulator system boosting the development procedures of the solar panel based devices offering an alternative, highly accurate and digitally customizable power source

replacing photovoltaic cells and simulating direct sunlight effects for indoor experiments.

In order to design such a system we need accurate modeling of the photovoltaic cell, and a versatile power supply which can cover the desired voltage-current range of the emulated solar array with good resolution and response time.

2. MODELING THE PHOTOVOLTAIC CELL

Basically four diode based models are known for proper modeling of the photovoltaic cells. The most accurate results are obtained [1] when using the double exponential model presented in figure 1.

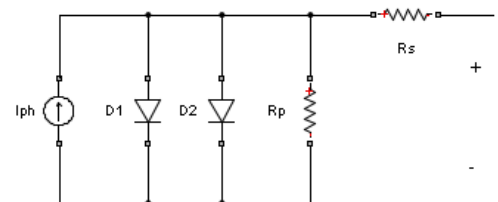


Fig. 1 The double exponential model

$$I = I_{ph} - (V + I * R_s) / R_p - \sum_{i=1}^2 I_{Si} * \left(e^{(V + I * R_s) / (N_i * V_t)} - 1 \right)$$

The following equation presents the double exponential model:

where:

- I_{ph} is the solar-induced current, temperature dependent

$$I_{ph} = I_{ph}(T_0) + K_0 \cdot (T - T_0); \quad (2)$$

- $I_{ph}(T_0)$ is the solar induced current at normalized temperature
 $T_0 = (273 + 25)[K]$,
- K_0 is the current-temperature coefficient in $[A/K]$
- I_{S1}, I_{S2} is the saturation current of the first and the second diode
- $V_t = \frac{kT}{q}$ is the thermal voltage, where
 k -is the Boltzmann constant, T -temperature of the photovoltaic cell, q -elementary charge of an electron
- N_1 and N_2 is the quality factor of the first and the second diode
- V is the voltage across the photovoltaic cell

The equation is a nonlinear problem which can be solved by numerical methods using Newton-Raphson method which successively approximates the roots of the equation. Calculating the roots of the equation in every step of the digital closed loop regulation is computationally intensive. These calculations need to be done offline on the host computer and the resulted data transferred back to the embedded system in order to have a fast control loop. In this case several current-voltage profiles are stored in the embedded system. The storage capability of the embedded system should be large enough to obtain high fidelity of the simulated photovoltaic cell. In case the CPU processing power is sufficiently high, or fast control loop is not desired, the numerical method can be used online. The authors obtained the different current-voltage and power-voltage characteristics for a single cell using a modified version of the script presented in [2].

3. THE SEPIC MODEL

In order to accurately model the solar array behavior over the whole output current and voltage range of interest we choose the SEPIC (Single Ended Primary Inductor Converter) converter topology, which from an input DC voltage that's above or beneath the desired output voltage gives positive regulated voltage on its output by controlling a single switching element (i.e. a MOSFET). Despite its need of having two inductors, this topology shows clear advantages in solar cell simulation. The series capacitor allows the converter to work in near-short-circuit conditions, conditions that are very much likely to occur when using a real solar cell or array. The SEPIC topology has been analyzed by several authors, a detailed mathematical analysis including state space equations are presented in [3], [4] a step by step design procedure, detailing passive and active component selections, is explained in [5], the modeling based on switching function and harmonic balance technique is presented in [6], detailing the voltage and current values based on duty cycle values on each passive component in the circuit. Our approach is, that based on the steady state

conditions, to develop a complete SIMULINK model to be used further in evaluating the solar array simulator.

3.1. The electrical and mathematical model

The basic schematic of the SEPIC converter is shown in figure 2a with MOSFET and diode as switching elements.

To simulate the behavior of a SEPIC converter, the traditional variable topology method was used. Switching elements got replaced with open-circuits and short circuits depending on the control input state. A common method for power transfer between input and output is by means of a PWM signal. This is generated by comparing a triangular waveform and a reference that can be fed back from the output or given constant.

The proposed model is based on a constant reference voltage, yielding a constant switch on-time. Given the bivalent nature of this comparison result, two steady circuit states can be identified. Replacing the semiconductors with open and short circuits accordingly will result in two possible electrical states: Q shorted, D open (figure 2b) and Q open, D shorted (figure 2c).

We use the following notations: i_{L1} - the current through L_1 inductor, i_{L2} - the current through L_2 inductor, v_{C1} - the voltage across C_1 capacitor, v_{C2} - the voltage across C_2 capacitor which is also equal to the output voltage V_{OUT} .

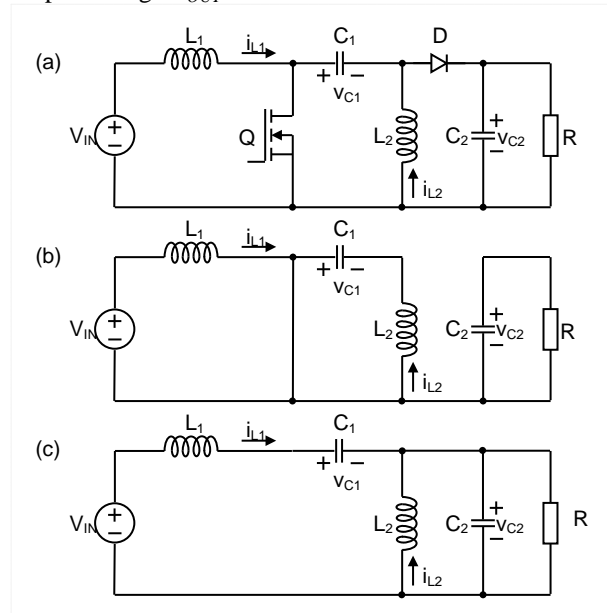


Fig 2. SEPIC converter (an ideal schematic): (a) practical realization with MOSFET and diode, (b) the case when the MOSFET conducts, (c) the case when the diode conducts.

Using Kirchhoff's laws and basic algebraic manipulations during both states depicted in figure 2a and figure 2b, we can deduce formulas for currents through capacitors and voltages across inductors, resulting in the following equations, where G is a digital signal, denoting when Q is in conduction mode:

$$v_{L_1} = G \cdot V_{IN} + \bar{G} (V_{IN} - v_{C_1} - v_{C_2}); \quad (3)$$

$$i_{C_1} = -G \cdot i_{L_2} + \bar{G} \cdot i_{L_1}; \quad (4)$$

$$v_{L_2} = G \cdot v_{C_1} - \bar{G} \cdot v_{C_2}; \quad (5)$$

$$i_{C_2} = -G \cdot \frac{v_2}{R} + \bar{G} \cdot \left(-\frac{v_2}{R} + i_{L_2} + i_{L_1} \right). \quad (6)$$

The voltages across the capacitors are expressed in equations (7) and (8), where i_{C_1} and i_{C_2} denotes the currents through C_1 and C_2 respectively:

$$v_{C_1} = \frac{1}{C_1} \cdot \int di_{C_1} \cdot dt; \quad (7)$$

$$v_{C_2} = \frac{1}{C_2} \cdot \int di_{C_2} \cdot dt. \quad (8)$$

We will use these equations to build the model of the converter in SIMULINK environment.

3.2. The SIMULINK model

The model of the SEPIC controller was developed using the steady state equations through standard SIMULINK mathematical blocks. The models for the energy storage elements (figure 3) consist of a gain and an integrator, voltages across capacitors and currents flowing through inductors are outputs of such subsystems. The same principles apply for all capacitors and inductors in the circuit.

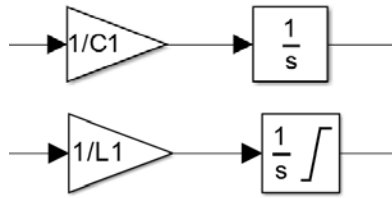


Fig. 3 Energy storage elements

The outputs of these blocks are fed back into the equations, with the voltage across C_2 being the output of the controller model. The model inputs are I_{OUT} (Output current), V_{IN} (Input voltage) the duty cycle and the triangular wave, the last two, along with the comparator block, determine the ON and OFF time of the switching element. The SEPIC converter was built using the blocks described above.

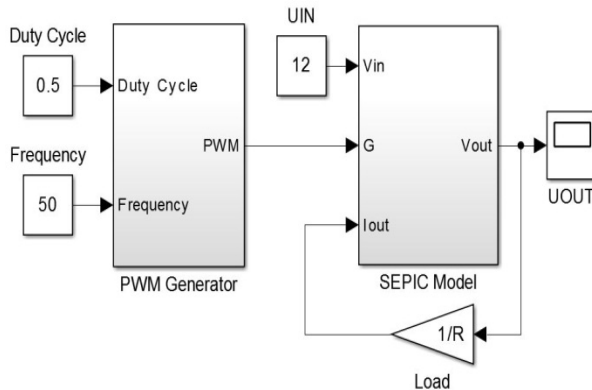


Fig. 4 The open-loop control system

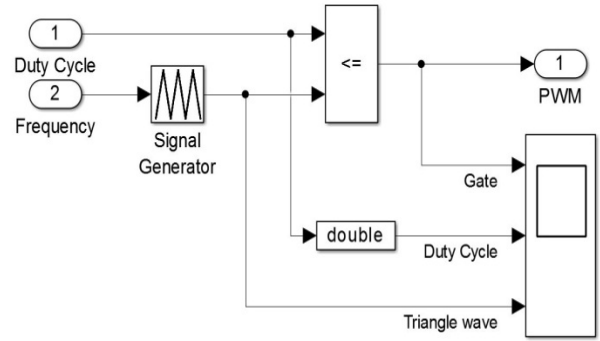


Fig. 5 The PWM generator

Figure 4 presents the Open-loop control system developed in SIMULINK environment, which consists of the PWM generator and SEPIC model.

The input to the model is the duty cycle and frequency, and the output of the model is the SEPIC's output voltage loaded with a resistor.

Figure 5 sketches the detailed SIMULINK model for the PWM Generator module. As before mentioned, the duty cycle is compared against a triangular wave, the comparison result will yield the PWM signal that will be applied to the control pin (gate) of the switching element.

Figure 7 is about the detailed SIMULINK model of the SEPIC converter topology, depicting all the connections described in the equations from (3) to (8). For better understanding of the interconnection links we use the notation $G=G1=G2=G3$.

4. SOLAR ARRAY SIMULATION

In order to validate our design we have modeled the different characteristics of the simulated solar array using the following parameters: Cell type: Q-Cells_Q6LMXP3 [7]; the open circuit voltage of a single cell $V_{oc}=0.637$ V; the short circuit current of a single cell $I_{sc}=9.17$ A; number of parallel cells=2; number of serial cells=20.

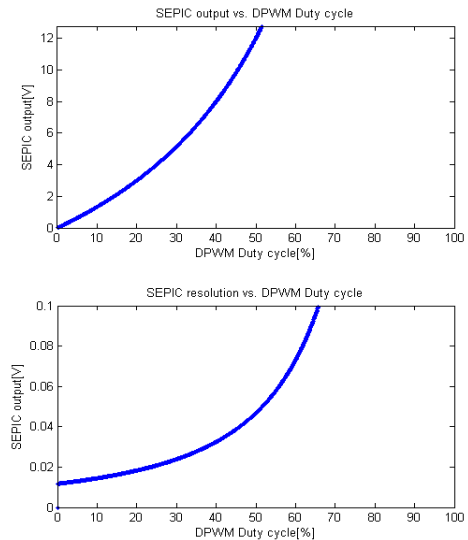


Fig. 6 SEPIC output and resolution

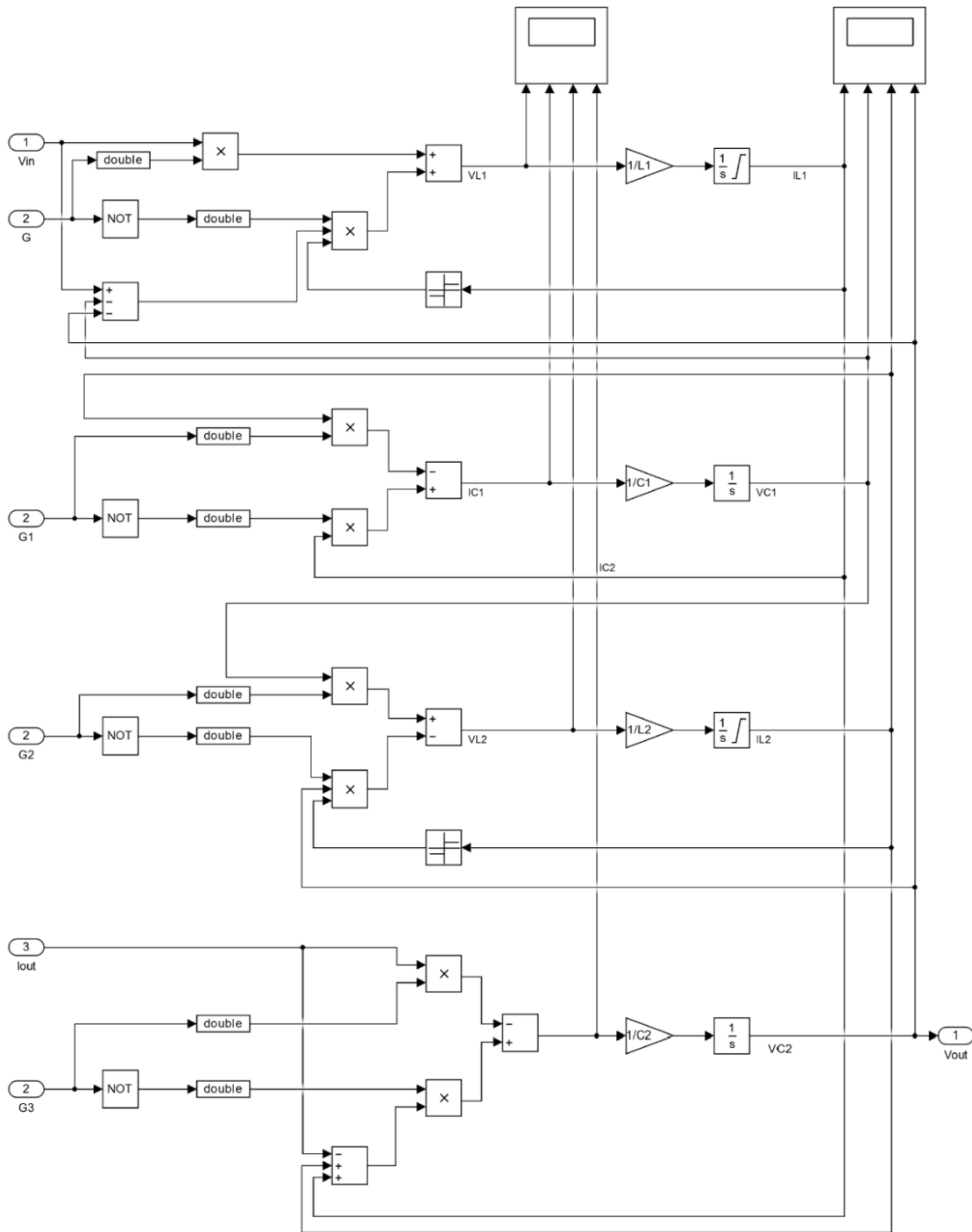


Fig. 7 The detailed model of the SEPIC converter

For the SEPIC converter we used the following settings: the input voltage $V_{in} = 12$ V; resolution of DPWM=10bit.

With the given serial-parallel configuration the SEPIC converter should be able to provide an output voltage range of 0-18.34 A and 0-12.74 V.

Figure 8 shows the voltage-current and voltage-power curves of the solar array simulator with the settings presented above with several different insolation and temperature settings. It can be observed that as the output voltage increases the achievable

resolution drops. This can observe in a better way if we look at the simulations in figure 6, which shows the SEPIC output voltage versus the duty of the DPWM control signal and the SEPIC output resolution versus the duty cycle of the DPWM signal.

We can also observe that the usable range of the duty cycle for the desired output voltage range is from 0 to 52%, which almost halves the initial resolution of the design because of the inherent nonlinear characteristic of the SEPIC converter.

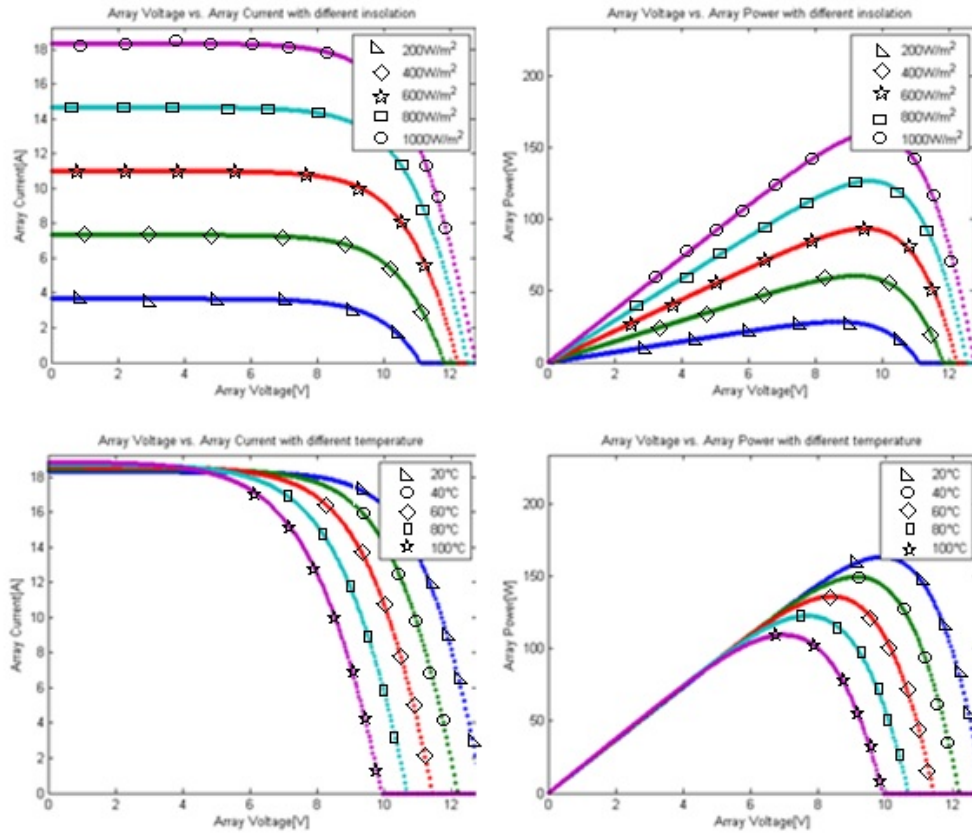


Fig. 8 Solar Array Characteristics

One of the project goals is to implement the simulator algorithm on a simple 8-bit RISC architecture MCU unit with USB capability. Thus, usually the maximum available instruction cycle frequency for a budgetary MCU is 12 MHz (given by the 48 MHz oscillator frequency), this instruction cycle speed will determine the switching frequency of the SEPIC converter for the required DPWM resolution. Having N bit resolution the following relationship:

$$f_{PWM} \leq \frac{f_{instr}}{2^N}. \quad (9)$$

needs to be fulfilled, where f_{PWM} is the switching frequency and f_{instr} is the CPU instruction frequency.

After analyzing the equation we can observe that the SEPIC converter's switching frequency should be less than or equal 11,718 kHz in order to achieve 10 bit resolution over the entire range of the possible duty cycle values. However, as it has been explained and presented in figure 6, since the usable range of the dutycycle values are almost halved, the effective, usable resolution will be only 9 bits.

In order to validate our simulation we compare the results from datasheet (figure 9) with our simulated results for a single cell (figure 10) under the same irradiation circumstances. We estimate that the overall differences are within $\pm 2\%$ of the datasheet values.

The simulated transient results in figure 11 show that the rise time of the SEPIC converter under the "worst" case situation is less than 5ms, which leads to

an acceptable closed control loop bandwidth for solar simulation applications.

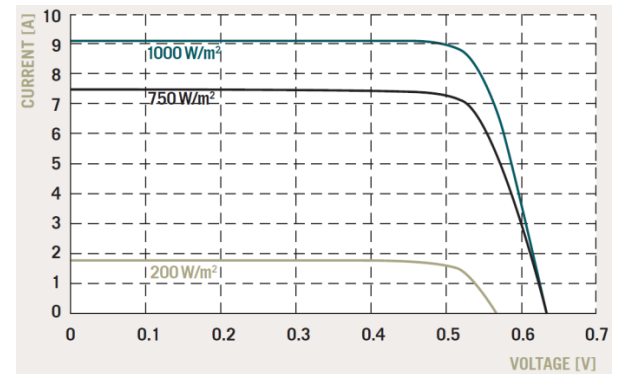


Fig. 9 Data from the Q-Cells_Q6LMXP3 datasheet

5. THE I-U CURVE TRACKING ALGORITHM

The electrical simulator should follow the inherent nonlinear characteristics of the photovoltaic array. Yuan Li et al [8] were presented a hybrid control strategy where the output parameter (current or voltage) regulation depends on the measurements (voltage and current) and a voltage based or current based control method is applied. For better results regarding output stability near MPPT (Maximum Power Point Regulation), regulation-point voltage control is preferred, based on the measured resistance, since using either pure voltage or current control will suffer an oscillation [8].

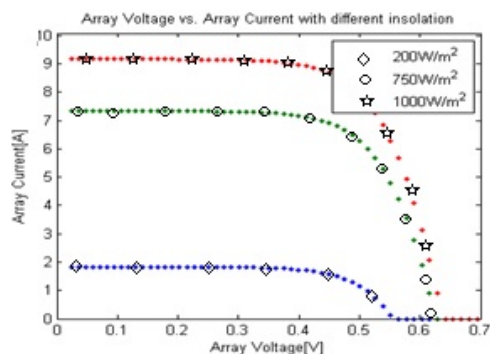


Fig. 10 The simulated results for a single cell

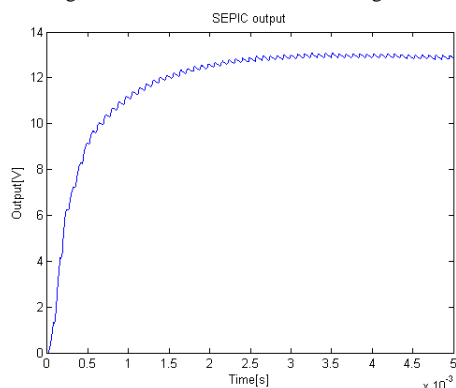


Fig. 11 The SEPIC transient simulation

Using this type of control in this case proves to be a stable solution since there is a unique resistance corresponding to every operation point on the PV curve and the reference voltage is stable when this control method applies. Since the output load-conditions of the electrical simulator are unpredictable, the closed loop controller must respond as quickly as possible to these load changes. The converter is regulating both the output voltage and current and depending on situations and the current position on the I-U curve, different strategies are used which control loop has higher priority.

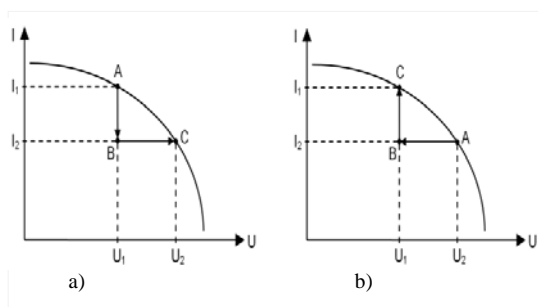


Fig. 12 a) Load increases; b) Load decreases

Assuming that the current and voltage values correspond to a point A on the I-U curve where $A=f(U,I)$, we can distinguish two different scenarios during an output load change.

In the first scenario the output load decreases, resulting in a decrease of the output current, the output voltage remains at the same level, the current limiting control loop is no longer active, only the voltage control loop is active. This will result in the converter

operating point moving from A to B. In order to follow the ideal I-U characteristic, the output voltage of the converter will be increased until the output voltage ramp and the $f(U,I)$ curve intersects. This will result in the converter operating point moving from B to C as shown in figure 12 a). In the second scenario, as the output load increases, the output current remains at the same level limited by the active current control loop. These are resulting in a decreased output voltage and thus the converter operating point will moving from A to B. In order to follow the ideal I-U characteristic, the output current of the converter will be increased until the output current ramp and the $f(U,I)$ curve intersects. This will result in the converter operating point moving from B to C (figure 12 b).

6. CONCLUSIONS

The authors developed a complete SIMULINK model of the SEPIC converter based on the equations in steady state. The paper highlights the main aspects to take in consideration when developing a solar array simulator, such as resolution problems typical to digital systems, control strategies because of the inherent nonlinear characteristics of both the SEPIC converter and the solar array I-U curves.

7. ACKNOWLEDGEMENT

This paper is supported by the Sectoral Operational Programme Human Resources Development (SOP HRD), ID134378 financed from the European Social Fund and by the Romanian Government.

REFERENCES

1. L. Turos, G. Csern  th and I. Szekely, "Embedded Photovoltaic Simulator System," in Proceedings of the 4th International Conference on Recent Achievements in Mechatronics, Automation, Computer Sciences And Robotics, Tirgu Mures, 2013.
2. G.-L. Francisco M., "Model of Photovoltaic Module in MATLAB," in Segundo Congreso Iberoamericano de estudiantes de Ingenieria Electrica, Electronica y Computacion,, 2005.
3. B. Schaeffer and D. Gilbert, "Analysis of the SEPIC Converter," 2010. [Online]. Available: http://web.cecs.pdx.edu/~tymerski/ece445/groups/SEPIC_analy sis_Team_2.pdf.
4. D. Zhang, "AN-1484 Designing A SEPIC Converter," Texas Instruments, 2013.
5. J. Falin, "Designing DC/DC converters based on SEPIC topology," Analog Applications Journal, 4Q 2008.
6. S. Taiwo and J. Y. Oricha, "Modeling, Steady-State Analysis of a SEPIC dc-dc Converter Based on Switching Function and Harmonic Balance Technique," Journal of Power and Energy Engineering, vol. 2, pp. 704-711, 2014.
7. Hanwha Q.Cells GMBH, [Online]. Available: https://www.q-cells.com/uploads/tx_abdownloads/files/Hanwha_Q.CELLS_G mbH_Data_sheet_Q6LMXP3-G2_2012-10_Rev01_EN_01.pdf.
8. L. Yuan, L. Taewon, P. Fang. Z. and L. Dichen, "A Hybrid Control Strategy for Photovoltaic Simulator," in Applied Power Electronics Conference and Exposition, 2009. APEC 2009. Twenty-Fourth Annual IEEE.